PHYSICAL REVIEW A VOLUME 45, NUMBER 4 15 FEBRUARY 1992

Polydispersity analysis of scattering data from self-assembled systems

Eric Y. Sheu
Texaco Research Center, P.O. Box 509, Beacon, New York 12508
(Received 22 August 1991)

A self-consistent method is proposed to treat the small-angle scattering data from polydispersed self-assembled systems. This method presumes a particle-size distribution to fit the scattering data, then calculates the averaged scattering contrast according to the presumed particle-size distribution. The scattering contrast should be independent of concentration, unless the presumed particle-size distribution function is not appropriate. Therefore performing this analysis as a function of concentration provides a way to self-consistently check the presumed distribution function. This method, although indirect, allows one to select a proper particle-size distribution and evaluate the system polydispersity. Seven commonly used distribution functions are discussed. In addition, the explicit forms of the intraparticle structure factor for these seven size-distribution functions were derived.

PACS number(s): 61.25.Hq

I. INTRODUCTION

The colloidal particles in a self-assembled system, such as micellar or microemulsion systems, often show significant polydispersity. This is a result of thermodynamic equilibrium, where the system free energy is minimized [1–5]. Since the particle polydispersity is governed by the system free energy (consisting of many free-energy terms), one may study the free energies via studying the particle-size distribution [5]. There have been many studies on polydispersity of various colloidal systems using different techniques. These include dynamic and static light scattering [6–12], differential mobility analyzer [13], and small-angle scattering [14–18]. Among them, light scattering has been a popular method. To obtain particle-size distribution from light-scattering data, one either inverts the correlation function directly [6,9], or presumes a particle-size distribution function and performs the cumulant analysis [9–12]. However, for systems that are not optically transparent, the light-scattering technique cannot be applied. For these cases, small-angle neutron scattering (SANS) or small-angle x-ray scattering (SAXS) techniques are often used [14,15]. Since the scattering kernel of SANS and SAXS is different from that of light scattering, the direct inversion method may not be obtained analytically. Numerical inversion, although achievable [19], imposes constraints which are not always appropriate. A widely used method is to presume a functional form for the particle-size distribution and calculate the scattering intensity accordingly [14,15], in order to fit the experimental data. Through this fitting the polydispersity information can be extracted. This method is plausible when the scattering intensity can be both measured and computed in an absolute scale (differential cross section per unit volume of sample). However, for cases such as crude oil systems or derivatives of fermentation broth, it is very difficult to compute the scattering intensity in the absolute scale, because the particle-solvent contrast often cannot be precisely computed. As a result, an adjustable amplitude parameter is often used to accommodate the scattering amplitude during the data fitting process. Due to this additional adjustable parameter, one may encounter multiple convergence in data fitting, and arrive at an ambiguous result.

In this paper, an analysis procedure was proposed to minimize the occurrence of multiple convergence. This procedure is for dilute systems where interparticle interactions are negligible. The procedure for more concentrated systems will be discussed in the future. This procedure consists of four steps: (1) presumption of a functional form for particle-size distribution, (2) calculation of scattering intensity distribution function, and fitting of the experimental data to extract structural and polydispersity parameters, (3) calculation of the averaged particle-solvent scattering contrast according to the presumed particle distribution function, using the extracted parameters, and (4) repeating steps (2) and (3) for different particle concentrations. If the calculated averaged particle-solvent contrast is independent of concentration, then the presumed particle-size distribution is proper, otherwise, it is not correct. This is because the contrast reflects only the difference of the "scattering power" between particles and the solvent, its value should be independent of concentration, once the functional form of the size distribution remains the same. Thus, if the deduced contrast exhibits dependence on concentration, this dependence most likely originates from the effect of the presumed functional form for particle-size distribution. Therefore the deduced average particle-solvent contrast as a function of particle concentration becomes an indicator (to be referred to as justification parameter, JP) for judging the presumed distribution function. Mathematically, this procedure amounts to providing a necessary condition as a constraint, by which one can judge the presumed function. Since JP is a deduced quantity, its functional form depends on the presumed particle-size distribution. In this paper we derive JP for both spherical and cylindrical particles (with polydispersity in the length only) and for

several commonly used particle-size distributions.

The intraparticle structure factors for both spherical and cylindrical systems, with polydispersity taken into account, were also derived. These explicit expressions of the intraparticle structure factors are important, because they substantially reduce the computation steps, and thus time. This is essential in the process of data fitting. Secondly, an explicit form will allow one to study the dependence of the scattering intensity on a certain variable, such as particle size, polydispersity, or the geometrical asymmetry of the particles.

This paper is organized as follows. In Sec. II a brief description of the scattering intensity is given. In Sec. III the analytical forms of both JP and the corresponding averaged intraparticle structure factors for seven commonly used distribution functions were given. This is followed by the demonstration of a simulated case using this method in Sec. IV to test the sensitivity and applicability of this method. An experimental example is given in Sec. V. We then discuss this method and the results obtained in Sec. VI together with the conclusions.

II. SCATTERING INTENSITY

The scattering intensity distribution $I(Q)$, $[Q=(4\pi/\lambda)\sin\theta$, θ is the scattering angle] represents the differential cross section per unit volume of the sample at a scattering angle θ. For a monodisperse system, it can be written as

$$I(\mathbf{Q})=N_p P(\mathbf{Q})S(\mathbf{Q}) \tag{1}$$

where N_p is the number density of the particles. $P(Q)$ is the intraparticle structure factor defined as

$$P(\mathbf{Q})=|F(\mathbf{Q})|^2=|\int d\mathbf{r}[\rho_p(\mathbf{r})-\rho_s]\exp(i\mathbf{Q}.\mathbf{r})|^2 \tag{2}$$

where $F(Q)$ is the particle form factor, $\rho_p(\mathbf{r})$ is the scattering length density (electron density in SAXS) at $\mathbf{r}$ from the center of mass of the particle, and ρ_s is the scattering length density of the solvent. $S(\mathbf{Q})$ is the interparticle structure factor, representing the interparticle interactions. For dilute systems the interparticle correlations are negligible and $S(\mathbf{Q})$ can be taken as unity. Since we discuss only the dilute cases in this study, $S(\mathbf{Q})$ will be taken as unity. With $S(\mathbf{Q})=1$, the intensity distribution becomes

$$I(Q)=N_p P(\mathbf{Q}) . \tag{3}$$

From Eq. (3) one can see that if the system contains spherical particles (where form factor is equal to $[3j_1(QR)/QR]^2$, R is the radius and j_1 is the first-order Bessel function), $I(Q)$ will be totally governed by the particle radius [16–18]. In analyzing the scattering data from such a system, one can fit the data with Eq. (3) and use particle radius as the adjustable parameter. This fitting is usually very simple.

However, it is much more complicated in analyzing the $I(Q)$ data from a polydisperse system where $I(Q)$ comprises contributions from particles of all sizes, i.e.,

$$I(\mathbf{Q})=\int P(\mathbf{Q},x)dN_p(x) \tag{4}$$

where x is the size parameter with polydispersity (e.g., radius for the spherical particles and length for the cylindrical particles). $N_p(x)$ is the number density of the particle of size x. By defining a normalized size-distribution function $f(x)$ as

$$f(x)dx=dN_p(x)/N_0 \tag{5}$$

with

$$\int f(x)dx=\int dN_p(N_0)^{-1}=1 , \tag{6}$$

$I(Q)$ becomes

$$I(Q)=\int P(Q,x)N_0 f(x)dx . \tag{7}$$

N_0 is the total number density of the particles. The intraparticle structure factor in Eq. (7) for a particle of size x, $P(Q,x)$, can be written as

$$P(\mathbf{Q},x)=(\Delta\rho)^2 G(\mathbf{Q},x)[V_p(x)]^2 \tag{8}$$

where $V_p(x)$ is the volume of the particle and $G(Q,R)$ is the scattering kernel. For a spherical particle, $G(Q,R)$ reads

$$G(Q,R)=[3j_1(QR)/QR]^2 \tag{9}$$

where R is the radius. For a cylindrical system, $G(\mathbf{Q},x)$ is, assuming the polydispersity is in particle length L only [19],

$$G(Q,L)=\int_0^1 d\mu\left[\frac{\sin(\mu QL/2)}{\mu QL/2}\right]^2 \times\left[\frac{2J_1(QR_l\sqrt{1-\mu^2})}{QR_l\sqrt{1-\mu^2}}\right]^2 \tag{10}$$

where R_l is the cross-sectional radius of the cylinder, and $\mu=\cos\theta$ is the directional cosine. Combining Eqs. (4), (5), (7), and (8), one obtains

$$I(Q)=(\Delta\rho)^2 N_0\langle V_p^2\rangle\langle\tilde{P}(Q)\rangle \tag{11}$$

where

$$\langle\tilde{P}(Q)\rangle=\frac{\int G(Q,x)V_p^2 f(x)dx}{\int V_p^2 f(x)dx} \tag{12}$$

is the normalized average intraparticle structure factor (i.e., $\langle\tilde{P}(0)\rangle=1$). $\langle V_p^2\rangle$ is the second moment of the particle volume.

For experimental purposes we write N_0 in terms of the weight percent concentration,

$$C_w=k\int V_p(x)N_0 f(x)dx =kN_0\langle V_p\rangle \tag{13}$$

where k is a proportional constant for converting N_0 to the weight percent concentration. Combining Eqs. (11)–(13) one gets

$$I(Q)=[(\Delta\rho)^2/k]C_w(\langle V_p^2\rangle/\langle V_p\rangle)\langle\tilde{P}(Q)\rangle \tag{14a}$$

$$=A\langle\tilde{P}(Q)\rangle . \tag{14b}$$

As shown in Eq. (14b), an adjustable parameter A is used to represent the prefactors [see Eq. (14a)], when one cannot compute all of the terms shown in Eq. (14a) precisely. Equation (14b) is the equation often used to fit the experimental data from which A and the structural parameters [R in Eq. (9) or L and R_l in Eq. (10)] are extracted. From Eqs. (14a) and (14b), the average particle-solvent contrast can easily be deduced from the extracted A and the structural parameters as

$$A_0=(\Delta\rho)^2/k \tag{15}$$

$$=(A/C_w)(\langle V_p\rangle/\langle V_p^2\rangle) . \tag{16}$$

As mentioned in Sec. I, A_0 should be independent of concentration, if the presumed size distribution is appropriate and no particle swelling or shrinkage occurs as concentration varies. This means that when the presumed particle-size distribution function is proper, one should be able to eliminate all the size distribution dependence from the extracted A by multiplying it by $(\langle V_p\rangle/\langle V_p^2\rangle)/C_w$ [see Eq. (16)]. Therefore, if the A_0 values so obtained for different concentrations are the same, one can claim that the presumed size distribution has a proper functional form. Otherwise, a new form is needed.

Since $\langle V_p\rangle$ and $\langle V_p^2\rangle$ depend on the presumed particle-size distribution, A_0 has different functional form for different particle-size distribution. We shall give the derivations of A_0's for various distribution functions in the following section.

III. DERIVATIONS OF JUSTIFICATION PARAMETERS AND $\langle \tilde{P}(Q)\rangle$

The analytical forms of A_0 and $\langle \tilde{P}(Q)\rangle$ for systems containing spherical particles are derived in this section. Seven commonly used distribution functions were chosen for derivation of A_0 and $\langle \tilde{P}(Q)\rangle$. The cylindrical cases are given in Appendix A.

A. Monodisperse case

The first moment of the particle size in this case is equal to the square root of the second moment, i.e., $\langle V_p\rangle=(4\pi/3)R^3=(\langle V_p^2\rangle)^{1/2}$. Hence the justification parameter A_0 can easily be derived using Eq. (16),

$$A_0=(A/C_w)(\langle V_p\rangle/\langle V_p^2\rangle)$$

$$=3A/(4\pi R^3C_w) . \tag{17}$$

The intraparticle structure factor $\langle \tilde{P}(Q)\rangle$ obtained has the following form:

$$\langle \tilde{P}(Q)\rangle=[3j_1(QR)/QR]^2 . \tag{18}$$

B. Exponential distribution

The exponential distribution function is defined as [see Fig. 1(a)]

$$f(R)=\beta\exp(-\beta R) . \tag{19}$$

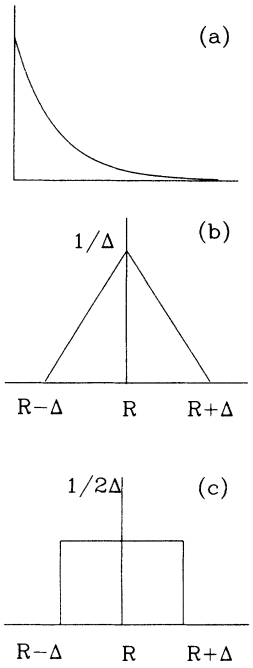

FIG. 1. (a) Normalized exponential distribution defined in $(0,\infty)$ with the first moment taken to be 25 Å [see Eq. (19)]; (a) Normalized triangular distribution defined in domain $[(R-\Delta),(R+\Delta)]$ [see Eq. (24)]; (b) normalized rectangular distribution defined in domain $[(R-\Delta),(R+\Delta)]$ [see Eq. (31)].

$\langle V_p\rangle$ and $\langle V_p^2\rangle$ in this case are, respectively,

$$\langle V_p\rangle=(4\pi/3)(3!/\beta^3) \tag{20}$$

and

$$\langle V_p^2\rangle=(4\pi/3)^2(6!/\beta^6) . \tag{21}$$

By Eqs. (16) and (12) one obtains, respectively,

$$A_0=A\beta^3/160\pi C_w \tag{22}$$

and

$$\langle \tilde{P}(Q)\rangle=\frac{\beta^6}{80Q^6}\left[\frac{1}{2}-\frac{\beta^2}{\eta}-\frac{Q\beta}{\eta}\sin(2\mathcal{E})+\frac{Q^2}{\beta^2}+\frac{Q^2\beta}{\eta^{3/2}}\cos(3\mathcal{E})\right] \tag{23}$$

where $\eta=\beta^2+4Q^2$ and $\mathcal{E}=\tan^{-1}(2Q/\beta)$.

C. Triangular distribution

The triangular distribution function can be expressed as [see Fig. 1(b)]

$$f(R)=\begin{cases}1/\Delta-(\bar{R}-R)/\Delta^2, & R\in[\bar{R}-\Delta,\bar{R}]\\ 1/\Delta-(R-\bar{R})/\Delta^2, & R\in[\bar{R},\bar{R}+\Delta]\\ 0 \text{ elsewhere} .\end{cases} \tag{24}$$

The first and second moments of V_p for this distribution function are, respectively,

$$\langle V_p \rangle = (8\pi\bar{R}/3)(\bar{R}^2+\Delta^2)+(\pi\bar{R}/3\Delta^2)\chi^4 \cdot$$

$$-(4\pi/15\Delta^2)\chi^5 , \quad (25)$$

and

$$\langle V_p^2 \rangle = (16\pi^2/63)[(\bar{R}/\Delta^2)\chi^7+(1/\Delta)(U^7+V^7)]$$

$$-(2\pi^2/3\Delta^2)\chi^8 , \quad (26)$$

where

$$U \equiv \bar{R}+\Delta, \quad V \equiv \bar{R}-\Delta ,$$

and (27)

$$\chi^i \equiv U^2+V^i-2\bar{R}^i .$$

By Eqs. (25) and (26) A_0 can be calculated by Eq. (15). By substituting this distribution function into Eq. (12) one obtains $\langle \tilde{P}(Q) \rangle$ to be

$$\langle \tilde{P}(Q) \rangle = (16\pi^2/Q^6\langle V_p^2 \rangle)$$

$$\times\{(1/\Delta)[M(U)-M(V)]-(2\bar{R}/\Delta^2)M(\bar{R})$$

$$-(1/\Delta^2)[N(U)-N(V)]+(2/\Delta^2)N(\bar{R})\} , \quad (28)$$

where

$$M(x) \equiv (Q^2R^3/6)+[(QR^2/4)-(5/8Q)]\sin(2QR)$$

$$+(3R/4)\cos(2QR)+R/2 , \quad (29)$$

and

$$N(x) \equiv [(QR^3/4)-(9R/8Q)]\sin(2QR)$$

$$+[(35R^2/8)-(21/16Q^2)]\cos(2QR)$$

$$+R^2/4+Q^2R^4/8 . \quad (30)$$

D. Rectangular distribution

The functional form of the distribution is [see Fig. 1(c)]

$$f(R) = \begin{cases} 1/2\Delta, & R \in [\bar{R}-\Delta, \bar{R}+\Delta] \\ 0 \quad \text{elsewhere} . \end{cases} \quad (31)$$

The $\langle V_p \rangle$, $\langle V_p^2 \rangle$, and $\langle \tilde{P}(Q) \rangle$ obtained for this distribution function are, respectively,

$$\langle V_p \rangle = (\pi/6\Delta)(U^4-V^4) , \quad (32)$$

$$\langle V_p^2 \rangle = (8\pi^2/63\Delta)(U^7-V^7) , \quad (33)$$

and

$$\langle \tilde{P}(Q) \rangle = (63/Q^6)[M(U)-N(V)]/(U^7-V^7) . \quad (34)$$

The JP in this case is

$$A_0 = (21A/16\pi C_w)[(U^4-V^4)/(U^7-V^7)] , \quad (35)$$

where U, V, M, and N have the same definitions as the triangular case.

E. Log-normal distribution

Log-normal distribution is convenient for describing the size distribution of polymeric systems, especially for interpretation of dynamic light-scattering data [10,12]. This is because it exhibits a number of properties that make it amenable to mathematical manipulations. This distribution function skews to the large particle size [see Fig. 2(a)]. It has the following form:

$$f(R) = (1/R\sqrt{2\pi}\ln z)\exp\{-[\ln(R/\bar{R})]^2/2\ln z\} \quad (36)$$

where $z = \bar{R}^2/\bar{R}^2 = \sigma^2+1$ (σ^2 is the standard deviation) is a measure of the standard deviation. The ith moment of this distribution function is

$$\langle M_i \rangle = (1/\bar{R}_i)\exp[i^2/2)\ln z] . \quad (37)$$

Thus $\langle v_p \rangle$ and $\langle V_p^2 \rangle$ for this case are, respectively,

$$\langle V_p \rangle = (4\pi/3)\langle M_3 \rangle \quad (38a)$$

and

$$\langle V_p^2 \rangle = (4\pi/3)^2\langle M_6 \rangle . \quad (38b)$$

The justification parameter is

$$A_0 = (3A/4\pi C_w)\bar{R}^3\exp(-27/2\ln z) . \quad (39)$$

The intraparticle structure factor for this case cannot be expressed explicitly and requires numerical integration.

F. Normal (Gaussian) distribution

Gaussian distribution is a natural result of a random process and is widely used. Gaussian distribution is symmetric with respect to the average size $\bar{R}$ [see Fig. 2(b)]. However, in a physical system the particle sizes are nonnegative. Thus the distribution has to be truncated at $R=0$. For such a case the Gaussian distribution function can be written as

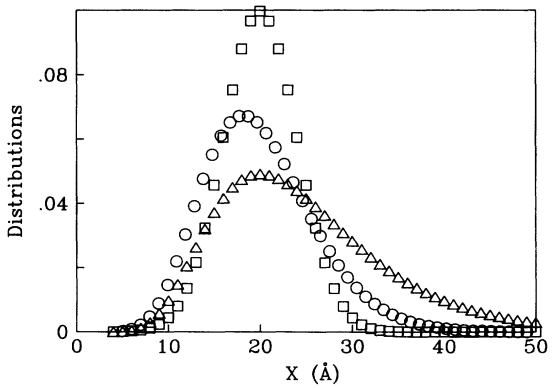

FIG. 2. (a) Normalized log-normal distribution (Δ) defined in $(0, \infty)$ [see Eq. (36)]; (b) normalized Gaussian distribution (□) defined in $(0, \infty)$ [see Eqs. (40) and (41)]; (c) Schultz distribution (o) defined by $\bar{X}$, the averaged particle size, and z, the width parameter characterizing the polydispersity through Eq. (47). The first moments for all three distribution functions were taken to be 20 Å. For Schultz distribution, z was taken to be 10.

$$f(R)=\alpha \exp[-(R-\bar{R})^2/2\sigma^2] \tag{40}$$

where

$$\alpha=(1/\sigma\sqrt{2}\pi)2[1-\phi(-\bar{R}/\sigma\sqrt{2})]^{-1} \tag{41}$$

is the prefactor to accommodate the normalization of $f(R)$ over $(0,\infty)$ range. Based on this modified Gaussian distribution $\langle V_p \rangle$ and $\langle V_p^2 \rangle$ are, respectively,

$$\langle V_p \rangle=(4\pi\alpha/3)\sigma^4\Gamma(4)D_{-4}(-\bar{R}/6)\exp(-3\bar{R}^2/4\sigma^2) \tag{42}$$

and

$$\langle V_p^2 \rangle=(16\pi^2\alpha/9)\sigma^7\Gamma(7)D_{-7}(-\bar{R}/6) \times \exp(-3\bar{R}^2/4\sigma^2) . \tag{43}$$

A_0 in this case is

$$A_0=(A/160\pi\sigma^3C_w)[D_{-4}(-\bar{R}/\sigma)/D_{-7}(-\bar{R}/\sigma)] . \tag{44}$$

Finally, letting $\beta^2=(\bar{R}-i2\sigma^2Q)^2/2\sigma^2$, $\gamma=\bar{R}/\sigma$, $\delta=\exp(\beta^2)$, and $g=1-\phi(\beta)$, one gets

$$\langle \tilde{P}(Q) \rangle=[3/4\sigma^6Q^6\Gamma(7)D_{-7}(-\gamma)]\exp(\gamma^2/4) \times\{2D_{-1}(-\gamma)\exp(-\gamma^4/4)-\sigma\sqrt{2\pi}\exp(-\gamma^2/2)\,\mathrm{Re}(\delta g)-4\sigma Q\sqrt{\pi}\exp(-\gamma^2/2)\,\mathrm{Im}(\beta g/\delta) +4Q^2\sigma^2D_{-3}(-\gamma)+4Q^2\sigma^2\exp[-(3\gamma^2+4Q^2\sigma^2)/4]\,\mathrm{Re}[D_{-3}(\beta)\exp(-iQ\bar{R})]\} . \tag{45}$$

$\phi(x)$ is again the probability integral, $\Gamma(x)$ is the gamma function, and $D_\iota(x)$ is the parabolic cylinder function (see Appendix B).

G. Schultz distribution

In determination of polymer molecular weight distribution in aqueous solutions, the Schultz distribution function is often applied [14,15,20,21]. It is a two-parameter, $(\bar{R},z)$, distribution function. $\bar{R}$ is the averaged particle radius and z is a width parameter characterizing the particle polydispersity. The Schultz distribution [see Fig. 2(c)] reads

$$f(R)=[R^z/\Gamma(z+1)][(z+1)/\bar{R}]^{z+1} \times \exp[-(z+1)R/\bar{R}] . \tag{46}$$

The polydispersity p, defined as

$$p\equiv(\langle R^2 \rangle-\langle R \rangle^2)^{1/2}/\langle R \rangle , \tag{47}$$

can be expressed in terms of z as

$$p=1/\sqrt{z}+1 . \tag{48}$$

$\langle V_p \rangle$, $\langle V_p^2 \rangle$, A_0, and $\langle \tilde{P}(Q) \rangle$ for this distribution are, respectively [14,15],

$$\langle V_p \rangle=(4\pi/3)[\Gamma(z+4)/\Gamma(z+1)][\bar{R}/(z+1)]^3 , \tag{49}$$

$$\langle V_p^2 \rangle=(4\pi/3)^2[\Gamma(z+7)/\Gamma(z+1)][\bar{R}/(z+1)]^6 , \tag{50}$$

$$A_0=(A/C_w)[\Gamma(z+4)/\Gamma(z+7)][(z+1)/\bar{R}]^3 , \tag{51}$$

and

$$\langle \tilde{P}(Q) \rangle=8\pi\alpha^{(z+1)}\{\alpha^{-(z+1)}-(4+\alpha^2)^{-(z+1)/2}\cos(\xi_1)+(z+1)(z+2)[\alpha^{-(z+3)}+(4+a^2)^{-(z+3)/2}\cos(\xi_3)] -2(z+1)(4+\alpha^2)^{-(z+2)/2}\sin(\xi_2)\} \tag{52}$$

where

$$\alpha\equiv z+1/Q\bar{R} \tag{53}$$

and

$$\xi_i\equiv(z+i)\tan^{-1}(2/\alpha) . \tag{54}$$

Having derived the analytical forms of A_0's for different distributions, we will present a theoretical example in the following section to demonstrate the sensitivity of this method using the dependence of A_0 on particle polydispersity as a criterion.

IV. THEORETICAL CASES

As mentioned in Sec. I, judging the particle-size distribution through fitting often encounters realistic difficulty. This is because one often can fit the data with many different particle-size distributions. In some cases, one can even fit with a completely different particle structure and size distribution. To evaluate the quality of the fit, a χ^2 value is often used as a criterion. However, the convergent χ^2 values obtained in polydispersity analysis of scattering data can be so close that using this value to differentiate the quality of the fit becomes dangerous. In

some cases, a visual comparison of the calculated curve and the experimental data becomes the better way to judge the fitting quality.

In this section, we shall demonstrate a case where a simulated scattering intensity distribution (using Gaussian distribution for particle-size distribution) can be fitted with a monodisperse cylindrical model. To do that, we simulated a series of scattering intensity spectra of different standard deviation σ, taking average radius to be 25 Å. The contrast $\Delta\rho$, k, and concentration C_w [see Eq. (14a)] were all taken to be unity. We then fitted these simulated curves by assuming particles to be cylindrical in shape and monodisperse in size. Figures 3(a)–3(c) show the results of these fittings. By comparing the simulated and the fitted curves, it is reasonable to say that the fittings are "acceptable," although the fittings at large Q are not as good. However, it is tolerable because in scattering experiment the statistics at large Q are normally not as good. With the fitting shown in Figs. 3(a)–3(c) one may conclude that the system contains cylindrical particles of narrow size distribution. However, if we apply the corresponding JP values as a function of the standard deviation [or equivalently, different C_w, see Eq. (44)], then it is obvious that the cylindrical model cannot be correct (see Fig. 4). This is because the true A_0 (calculated from the given parameters) as a function of σ, in the case of a Gaussian distributed sphere, should be monotonically decaying (to be addressed in the discussion section), but it is monotonically increasing for the monodisperse cylindrical model. This distinctive

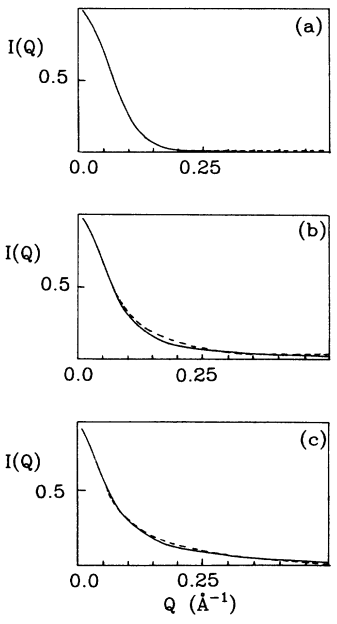

FIG. 3. Fittings of a series of Gaussian distribution simulated scattering intensity distributions (solid lines) with monodispersed cylindrical model (dashed lines): (a) $\sigma/\bar{R}=0.2$, (b) $\sigma/\bar{R}=0.5$, and (c) $\sigma/\bar{R}=0.7$. The fitting qualities are reasonable, indicating that using fitting quality for judging the structure and polydispersity is insufficient and is likely to lead to ambiguous results.

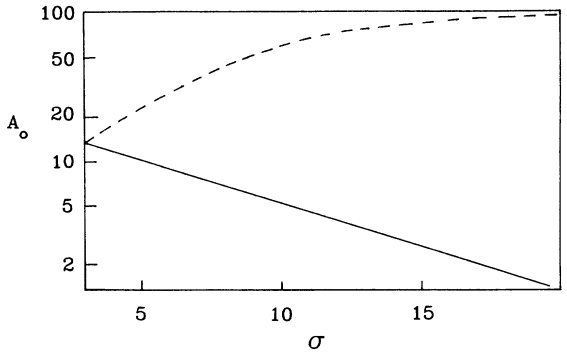

FIG. 4. A_0 of Gaussian distribution model (solid line) and that calculated from the monodisperse cylindrical model (dashed line) fittings as a function of particle polydispersity (in terms of standard deviation). It is obvious that the monodisperse cylindrical model is not correct because A_0 of the monodisperse cylindrical model behaves very differently.

difference indicates that this method can actually differentiate different distribution functions with a reasonable degree of sensitivity, even though their fitting qualities are similar.

V. EXPERIMENTAL APPLICATION

For an experimental test we applied this method to a series of SANS data for polydispersed microemulsion systems. This model system is a bis(2-ethyl) hexylsulfosuccinate (AOT)-water-decane three-component water-in-oil microemulsion system with AOT (g) to water (cm^3) maintained at 3:3 ratio. It has been proven, through electron microscopy studies [22] and absolute intensity SANS studies [14,15], that this system forms spherical microemulsion droplets, and the particle-size distribution follows a Schultz distribution function. In applying the JP method, we fitted the SANS data with various presumed particle distribution functions. From these fittings we found that both the spherical Schultz model and the monodisperse cylindrical model can fit the data (spherical Gaussian cannot fit well because the particle-size distribution turns out to be highly skewed to the right). The fittings are depicted in Figs. 5(a) and 5(b) for two concentrations. As mentioned in the preceding section, the χ^2 values for these two models are too close (1.11 and 1.13, respectively) to be used for evaluating their fitting qualities. By visual comparison, it is fair to say that both fittings are reasonable. In order to determine which of these two models describes the system polydispersity better, we plotted A_0 as a function of concentration (see Fig. 6). It is clear that the spherical Schultz model is a more appropriate model, because A_0 is nearly independent of the concentration. In addition, we found that A_0 values are relatively insensitive to temperature. This is predictable, because A_0 represents the average particle-solvent (water to decane) contrast, which should not vary substantially as a function of temperature, unless the particles swell or shrink. Actually, one can estimate the swelling of the particle through tempera-

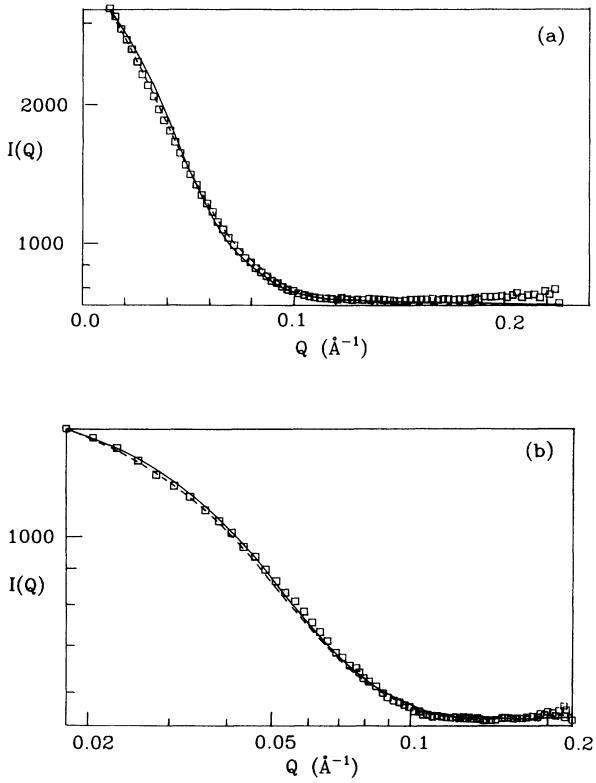

FIG. 5. Fittings of 3:3 (see text) AOT-water-decane microemulsion systems at different water droplet (including the AOT layer) volume fractions: (a) volume fraction equals 0.073 and (b) 0.11. The data (□) can be fitted with both the polydisperse (Schultz distribution) spherical model (solid line) and the monodisperse cylindrical model (dashed line). (a) and (b) were plotted as a function of Q and $\ln(Q)$, respectively, in order to detail the fitting at the different Q ranges.

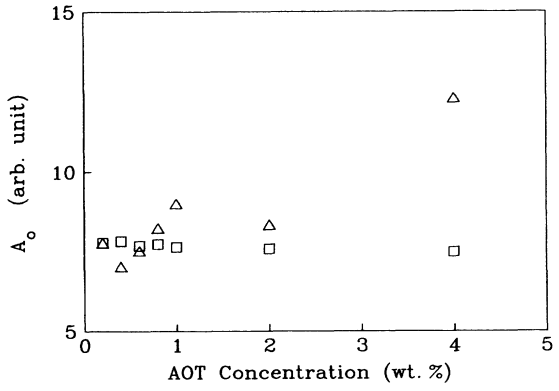

FIG. 6. A_0 values as a function of AOT surfactant concentration. The A_0 values of the Schultz spherical model (□) fluctuate around the mean value by less than 2% while the values of the monodisperse cylinder model (△) show a deviation of ~25%. This demonstrates the applicability of the justification method proposed here.

ture dependence of A_0 once the particle-size distribution function is determined.

VI. DISCUSSION AND CONCLUSIONS

The theoretical case we showed in Sec. IV is along the σ axis unlike the one we suggested (i.e., C_w axis). This is because the JP method is applicable only when the behavior of the polydispersity variables (such as $\bar{R}$ and σ in the case of Gaussian distribution) along the selected axis is either known or predictable. In the simulated case in Sec. IV, both $\bar{R}$ and σ depend on C_w, but their dependences on the C_w axis were not known. Thus it is difficult to simulate along the C_w axis. Essentially, the σ axis and the C_w axis are equivalent mathematically, because the statistical variables (i.e., $\langle V_p \rangle$ and $\langle V_p^2 \rangle$) in $I(Q)$ depend on both axes except that the dependence of $I(Q)$ on σ is direct while that on C_w is indirect. Thus using the σ axis to test the method is essentially the same as using the concentration axis. The only difference is that A_0 is not independent of σ. Therefore the test can only be achieved when the correct dependence of A_0 on σ (or the right particle distribution function) is known; this was the case in our theoretical demonstration in Sec. IV.

From the theoretical and the experimental demonstrations one sees clearly that using fitting quality as a criterion to extract the structure and polydispersity information from scattering data is insufficient and is likely to lead to incorrect results.

In this papaer we also derived the averaged particle form factor $\langle \tilde{P}(Q) \rangle$ for these distribution functions. These analytical expressions of $\langle \tilde{P}(Q) \rangle$ allow us to reduce the computation steps in the course of data fitting. In the derivation of these expressions, two special functions were involved, namely, the probability integral function and the parabolic cylinder function. They can be approximated by certain algebraic equations with reasonable accuracy [23]. In Appendix B the approximate algebraic equations for the parabolic cylinder function are given.

The effect of interparticle interactions on polydispersity has been discussed both theoretically and experimentally by many authors [24–27]. In general, the effect of interaction on the polydispersity, to the first-order approximation, is not appreciable, especially in the case of cylindrical particle systems as argued by Onsager [24], Ben-Shaul and Gilbart [25], and Blankschtein, Thurston, and Benedek [26]. Thus in treating the scattering data of an interacting system one can approximate $\langle S(Q) \rangle$ with a monodisperse model, using average radius $\bar{R}$ as the particle radius (in the spherical system). If this approximation is plausible, then the functional forms of A_0's given in this study will be applicable.

Since A_0 (equivalent to the averaged particle-solvent contrast) is inversely proportional to the particle density (while in solvent), one can make use of the A_0 value to study the swelling (or shrinkage) of the particles. For example, one can examine A_0 as a function of temperature to investigate how the solvent quality varies upon heating.

Recently, the maximum entropy method (MEM) was

developed by Skilling and Bryan [28]. It was based on Jayne's argument [29], which states that the only unprejudiced assignment which can be made for a discrete probability distribution $\{p_\iota\}$ is the one which has the maximum entropy S subject to the available information. Entropy here is defined in an information-theoretic sense to be $S=-\Sigma_\iota[p_\iota \ln(p_\iota)]$. This method has been widely applied to analysis of scattering data [30]. It gives a unique solution to the linear inverse problem. The particle-size distribution thus obtained is usually the most uniform one that is compatible with the data. However, its accuracy depends on the resolution in the measurement and the particle size as well [31,32]. Thus, to enhance the applicability of this method, knowledge about the resolution as a function of the particle size is necessary. We do not intend to compare JP method with MEM. We simply suggested that the JP method is one of the methods for polydisperse analysis, and the sensitivity in differentiating different models is reasonably good.

ACKNOWLEDGMENTS

The author would like to acknowledge Y. Shen for assistance in preparing part of the figures. The grant of neutron beam time on the H-9 small-angle-scattering spectrometer from Brookhaven National Laboratory and the expert assistance from Dr. D. K. Schneider are gratefully acknowledged. The author also thanks Exxon Research and Engineering Company, where part of this work was completed, for supporting this research during his stay.

APPENDIX A

In this appendix, we will give the expressions of $\langle V_p \rangle$, $\langle V_p^2 \rangle$, A_0, and $\langle \tilde{P}(Q) \rangle$ for cylindrical systems. The polydispersity is assumed to be in length of the cylinders while R_l, the cross-sectional radius, is taken as a constant for all particles. As defined previously [Eqs. (10) and (12)], the normalized averaged intraparticle structure factor reads

$$\langle \tilde{P}(Q) \rangle = \frac{\int V_p^2 G(Q,L) f(L) dL}{\int V_p^2 f(L) dL} \tag{A1}$$

where [see Eq. (10)]

$$G(Q,L) = \int_0^1 d\mu \left[\frac{\sin(\mu QL/2)}{\mu QL/2} \right]^2 \times \left[\frac{2J_1[QR_l(1-\mu^2)^{1/2}]}{QR_l(1-\mu^2)^{1/2}} \right]^2 \tag{A2}$$

$$\equiv \int_0^1 [\sin(\mu QL/2)/(\mu QL/2)]^2 \mathcal{R}^2 d\mu \tag{A3}$$

with

$$\mathcal{R} \equiv 2J_1[QR_l(1-\mu^2)^{1/2}]/QR_l(1-\mu^2)^{1/2} . \tag{A4}$$

Since the second term, R, of the integrand is independent of L and $V_p = \pi \mathcal{R}_l^2 L$, we can factor out this term from the integration with respect to L. By doing so, $\langle \tilde{P}(Q) \rangle$ can be written as

$$\langle \tilde{P}(Q) \rangle = \int_0^1 d\mu \, \mathcal{R}^2 \frac{4K_1(\mu Q)}{(\mu Q)^2 K_2(\mu Q)} \tag{A5}$$

where

$$K_1(Q\mu) = \int_0^\infty dL \, 4L^2 [\sin(\mu QL/2)/(\mu QL/2)]^2 f(L) \tag{A6}$$

and

$$K_2(Q\mu) = \int_0^\infty dL \, L^2 f(L) . \tag{A7}$$

Since the integrand in Eq. (A5) cannot be integrated with respect to μ analytically, the integration has to be performed numerically. However, K_1 and K_2 can be obtained analytically for the distribution functions used in Sec. III except for the case of log-normal distribution function. The advantage to expressing $\langle \tilde{P}(Q) \rangle$ in terms of K_1 and K_2 is that the derivations of K_1 and K_2 can be checked by taking $Q\mu \to O$ where K_1 should reduce to K_2. In the following we shall give the derivations of $\langle V_p \rangle$, $\langle V_p^2 \rangle$, K_1, K_2, $= (\pi R_l)^2 \langle V_p^2 \rangle$, and $\langle \tilde{P}(Q) \rangle$ for various distribution functions.

1. Monodisperse case

In a monodisperse system $f(L) = \delta(L - \bar{L})$ where $\delta(x)$ is the Kronecker delta function. In this case A_0 can be easily derived to be

$$A_0 = A/(\pi R_l^2 L C_w) \tag{A8}$$

and

$$\langle \tilde{P}(Q) \rangle = \int_0^1 d\mu \, \mathcal{R}^2 \left[\frac{\sin(\mu QL/2)}{\mu QL/2} \right]^2 . \tag{A9}$$

2. Exponential distribution

$$\langle V_p \rangle = \pi R_l^2/\beta , \tag{A10}$$

$$\langle V_p^2 \rangle = 2(\pi R_l^2/\beta)^2 , \tag{A11}$$

$$A_0 = A\beta/2\pi R_l^2 C_w , \tag{A12}$$

$$K_1 = (\mu Q)^2/[2(\mu^2 Q^2 + \beta^2)] , \tag{A13}$$

$$\langle \tilde{P}(Q) \rangle = \int d\mu \, \mathcal{R}^2 \{\beta^2/[\beta^2 + (\mu Q)^2]\} . \tag{A14}$$

3. Triangular distribution

$$\langle V_p \rangle = \pi R_l^2 \bar{L} , \tag{A15}$$

$$\langle V_p^2 \rangle = (\pi R_l^2)^2 [\bar{L}^2 + \Delta^2/6)] , \tag{A16}$$

$$A_0 = A\bar{L}/[\pi R_l^2 C_w (\bar{L}^2 + \Delta^2/6)] , \tag{A17}$$

$$K_1 = \tfrac{1}{2} - 2/(\mu Q\Delta)^2 \cos(\mu Q\bar{L}) \sin^2(\mu Q\Delta/2) , \tag{A18}$$

$$\langle \tilde{P}(Q)\rangle = \frac{12\Delta^2}{6\bar{L}^2+\Delta^2} \times \int_0^1 d\mu \mathcal{R} \times \left[\frac{(\mu Q\Delta)^4 - 4\cos(\mu Q\bar{L})\sin^2(\mu Q\Delta/2)}{(\mu Q\Delta)^4} \right] . \quad \text{(A19)}$$

4. Rectangular distribution

$$\langle V_p\rangle = \pi R_l^2 \bar{L} , \quad \text{(A20)}$$

$$\langle V_p^2\rangle = (\pi R_l^2)^2[\bar{L}^2 + (\Delta^3/3)] , \quad \text{(A21)}$$

$$A_0 = A\bar{L}/[\pi R_l^2 C_w^2(\bar{L}^2+\Delta^3/3)] , \quad \text{(A22)}$$

$$K_1 = \tfrac{1}{2}[1-\cos(\mu QL)\sin(\mu Q\Delta)/(\mu Q\Delta)] , \quad \text{(A23)}$$

$$\langle \tilde{P}(Q)\rangle = \frac{6\Delta^2}{3\bar{L}^2+\Delta^2} \times \int_0^1 d\mu \mathcal{R}^2 \times \left[\frac{(\mu Q\Delta) - \cos(\mu Q\bar{L})\sin(\mu Q\Delta)}{(\mu Q\Delta)^3} \right] . \quad \text{(A24)}$$

5. Log-normal distribution

Since the polydispersity is in the L direction only, $\langle V_p\rangle$ and $\langle V_p^2\rangle$ are equivalent to the first and the second moments of the distribution with prefactors being πR_l^2 and $(\pi R_l^2)^2$, respectively.

$$\langle V_p\rangle = \pi R_l^2/\bar{L}\exp[\tfrac{1}{2}\ln z] , \quad \text{(A25)}$$

$$\langle V_p^2\rangle = (\pi R_l^2\bar{L})^2\exp[(2\ln z)] , \quad \text{(A26)}$$

$$A_0 = (A/Cw\pi R_l^2\bar{L})\exp[(-3\ln z)/2] . \quad \text{(A27)}$$

They analytical form for K_1 cannot be obtained, thus $\langle \tilde{P}(Q)\rangle$ should be computed numerically by performing double integration.

6. Gaussian distribution

$$\langle V_p\rangle = (\pi R_l^2)[\bar{L} + \alpha\sigma^2\exp(-\bar{L}^2/2\sigma^2)] \quad \text{(A28)}$$

where α is the accommodation factor so that the Gaussian distribution is defined in the domain $(0, \infty)$. With this modification the $\bar{L}$ again becomes the most probable value of $f(L)$ and the first moment can be expressed in terms of $\bar{L}$ as

$$\langle L\rangle = \bar{L} \pm \alpha\exp(-\bar{L}^2/2\sigma^2) , \quad \text{(A29)}$$

$$\langle V_p^2\rangle = (\pi R_l^2)^2[\bar{L}^2+\sigma^2+2\alpha\sigma^2\bar{L}\exp(-\bar{L}^2/2\sigma^2)] , \quad \text{(A30)}$$

$$K_1 = \tfrac{1}{2}(1-\alpha T) , \quad \text{(A31)}$$

where

$$T = (\pi/8)^{1/2}e^{-(\mu Q)^2/2} \times \{2\cos(\mu Q\bar{L}) - [e^{i\mu Q\bar{L}}\phi(-\gamma_+) + e^{-i\mu Q\bar{L}}\phi(-\gamma_-)]\} \quad \text{(A32)}$$

with $\gamma_\pm = (1/\sqrt{2})(\bar{L}/\sigma \pm i\mu Q\sigma)$ and $\phi(x)$ being the probability integral (see Appendix B). The justification parameter becomes

$$A_0 = \frac{A[\bar{L}+\alpha\sigma^2\exp(-\bar{L}^2/2\sigma^2)]}{\pi R_l^2 C_w[\bar{L}^2+\sigma^2+2\alpha\sigma^2\bar{L}\exp(-\bar{L}^2/2\sigma^2)]} \quad \text{(A33)}$$

and

$$\langle \tilde{P}(Q)\rangle = \int_0^1 d\mu R^2 \times \frac{2-(\alpha\sigma\sqrt{2}\pi)[\cos(\mu Q\bar{L}) + \mathrm{Re}(\mathcal{G})]}{(\mu Q)^2[\bar{L}^2+\sigma^2+2\alpha\sigma^2\bar{L}\exp(-\bar{L}^2/2\sigma^2)]} \quad \text{(A34)}$$

where

$$\mathcal{G} = \phi[(\bar{L}/\sigma\sqrt{2}) + i(\mu Q\sigma/\sqrt{2})]\exp(i\mu Q\bar{L}) . \quad \text{(A35)}$$

7. Schultz distribution

$$\langle V_p\rangle = \pi R_l^2\bar{L} , \quad \text{(A36)}$$

$$\langle V_p^2\rangle = (\pi R_l^2\bar{L})^2[(z+2)/(z+1)] , \quad \text{(A37)}$$

$$A_0 = (z+1)A/(z+2)\pi R_l^2\bar{L}C_W , \quad \text{(A38)}$$

$$K_1 = \tfrac{1}{2}(1-T) \quad \text{(A39)}$$

where

$$T = \left[\frac{(z+1)^2}{(\mu Q\bar{L})^2+(z+1)^2} \right]^{(z+1)/2} \cos\{(z+1)\arctan[\mu Q\bar{L}/(z+1)]\} , \quad \text{(A40)}$$

$$\langle \tilde{P}(Q)\rangle = \frac{2Z}{Z+1}\int_0^1 d\mu \mathcal{R}^2 \frac{1-[Z^2/Z^2+(\mu Q\bar{L})^2]^{Z/2}\cos[Z\tan^{-1}(\mu Q\bar{L}/Z)]}{(\mu Q\bar{L})^2} \quad \text{(A41)}$$

where $Z = z+1$.

APPENDIX B

The analytical forms of both A_0's and $\langle \tilde{P}(Q) \rangle$ derived in this study involved three special functions namely, the gamma function $\Gamma(x)$, the parabolic cylinder function $D_\nu(x)$, and the probability integral $\phi(x)$. The advantage of using these special functions is that they can be approximated by algebraic functions with considerable accuracy, which makes the computation simpler and faster. In the following, we shall give the approximation forms for these three special functions and the recurrence relations between them.

The Γ function is a commonly used function which computed rather easily. A computer program in FORTRAN is available [33]. The parabolic cylinder function discussed here, $D_\nu(x)$, comes from the solution of the differential equation [23]

$$(d^2y/dx^2)-(\tfrac{1}{4}x^2+a)y=0 \ . \tag{B1}$$

This equation has an even (ξ_1) and an odd (ξ_2) solution. D_ν can be expressed in terms of ξ_1 and ξ_2, through Y_1 and Y_2, as

$$D_{-a-1/2}=Y_1\cos[(\tfrac{1}{4}+a/2)\pi]-Y_2\sin[(\tfrac{1}{4}+a/2)\pi] \tag{B2}$$

where

$$Y_1=(1/\sqrt{\pi})[\Gamma(\tfrac{1}{4}-a/2)/2^{a/2+1/2}]\xi_1 \ , \tag{B3}$$

$$Y_2=(1/\sqrt{\pi})[\Gamma(\tfrac{3}{4}-a/2)/2^{a/2-1/2}]\xi_2 \ , \tag{B4}$$

and

$$\xi_1=e^{-x^2/4}\left[1+(a+\tfrac{1}{2})\frac{x^2}{2!}+(a+\tfrac{1}{2})(a+\tfrac{5}{2})\frac{x^4}{4!}+\cdots\right] \tag{B5}$$

and

$$\xi_2=e^{-x^2/4}\left[x+(a+\tfrac{3}{2})\frac{x^3}{3!}+(a+\tfrac{3}{2})(a+\tfrac{7}{2})\frac{x^5}{5!}+\cdots\right] \tag{B6}$$

are convergent series for all x. With these algebraic equations $D_\nu(x)$ can be computed in a straightforward manner.

The probability integral is defined as [34]

$$\phi(x)=\frac{2}{\sqrt{\pi}}\int_0^x dt\, e^{-t^2} \ . \tag{B7}$$

Since $\phi(x)$ is defined in a finite domain for a given x, one can easily perform this integration.

[1] J. N. Israelachivili, D. J. Mitchell, and B. W. Ninham, J. Chem Soc. Faraday Trans. II **72**, 1525 (1976).
[2] B. Owenson and R. Pratt, J. Phys. Chem. **88**, 2905 (1984).
[3] E. Y. Sheu and S. H. Chen, J. Phys. Chem. **92**, 4466 (1988).
[4] R. J. M. Tausk and J. Th. G. Overbeek, Biophys. Chem. **2**, 53 (1974).
[5] P. J. Missel, N. A. Mazer, G. B. Benedek, C. Y. Young, and M. C. Carey, J. Phys. Chem. **84**, 1044 (1980).
[6] M. Bertero and E. R. Pike, Opt. Acta **30**, 1043 (1983); M. Bertero, P. Boccacci, and E. R. Pike, Proc. R. Soc. London, Ser. A **383**, 15 (1982).
[7] M. Bertero, P. Boccacci, and E. R. Pike, Inverse Problems **1**, 111 (1985).
[8] C. Wu, W. Buck, and B. Chu, Macromolecules **20**, 98 (1987).
[9] See, for example, *Measurement of Suspended Particles by Quasielastic Light Scattering,* edited by B. E. Dahneke (Wiley, New York, 1983); *Modern Methods of Particle Size Analysis,* edited by H. Barth (Wiley, New York, 1984).
[10] J. C. Thomas, J. Colloid Interface Sci. **117**, 187 (1987).
[11] A. K. Livesey, P. Licinio, and M. Delaye, J. Chem Phys. **84**, 5102 (1986).
[12] G. R. Strobl, J. Appl. Crystallogr. **6**, 365 (1973); P. Licinio and M. Delaye, J. Colloid Interface Sci. **132**, 1 (1989).
[13] C. Roth, U. Berlauer, and J. Heyder, J. Aerosol Sci. **20**, 547 (1989).
[14] M. Kotlarchyk and S. H. Chen, J. Chem. Phys. **79**, 2461 (1983); M. Kotlarchyk, S. H. Chen, J. S. Huang, and M. W. Kim, Phys. Rev. A **29**, 5054 (1984).
[15] R. B. Stephen, J. Appl. Phys. **61**, 1348 (1987).
[16] G. Porod, in *Small Angle X-Ray Scattering,* edited by O. Glatter and O. Kratky (Academic, New York, 1982).
[17] A. Guinier and G. Fournet, *Small Angle Scattering of X-Ray* (Wiley, New York, 1955).
[18] B. Jacrot, Rep. Prog. Phys. **30**, 911 (1976).
[19] O. Glatter, J. Appl. Crystallogr. **10**, 415 (1977).
[20] B. H. Zimm, J. Chem. Phys. **16**, 1099 (1948).
[21] N. C. Ford, Jr., R. Gabler, and F. E. Karasz (unpublished).
[22] W. Jahn and R. Strey, J. Phys. Chem. **92**, 2294 (1988).
[23] *Handbook of Mathematical Functions with Formulas, Graphs, and Mathematical Tables,* edited by M. Abramowitz and I. Stegun, Natl. Bur. Stand. (U. S.) Appl. Math. Ser. No. 55 (U. S. GPO, Washington, DC, 1972), p. 686.
[24] L. Onsager, Ann. N. Y. Acad. Sci. **51**, 627 (1949).
[25] A. Ben-Shaul and W. M. Gilbart, J. Phys. Chem. **86**, 316 (1982).
[26] D. Blankschtein, G. M. Thurston, and G. B. Benedek, J. Chem. Phys. **85**, 7268 (1986).
[27] C. Tanford, *The Hydrophobic Effect* (Wiley, New York, 1980).
[28] J. Skilling and R. K. Bryan, Mon. Not. R. Astron. Soc. **211**, 111 (1984).
[29] E. T. Jaynes, Phys. Rev. **106**, 620 (1957).
[30] R. L. Parker, Rev. Earth Planet. Sci. **5**, 272 (1977); J. A. Potting, G. J. Daniell, and B. D. Rainform, J. Appl. Crystallogr. **21**, 891 (1988).
[31] J. A. Potting, G. J. Daniell, and B. D. Rainford, J. Appl.

Crystallogr. **21**, 663 (1988).
[32] P. Thiyagarajan (private communication).
[33] W. H. Press, B. P. Flannery, S. A. Teukolsky, W. T. Vetterling, *Numerical Recipes* (Cambridge University Press, New York, 1987), p. 156.
[34] I. S. Gradshteyn and I. M. Ryzhik, *Table of Integrals, Series, and Products,* edited by A. Jeffrey (Academic, New York, 1980).